Simultaneous Removal of NO, SO2 and Hg0 with the WDRMRS

Mingqiang Deng
Donghua University
Zhengguo Xiao
Shanghai Textile Research Institute CO. Ltd
Dengxin Li (lidengxin@dhu.edu.cn)
Donghua University Songjiang Campus
Qiaoling Zhu
Donghua University - Songjiang Campus: Donghua University
Qin Chen
Donghua University - Songjiang Campus: Donghua University
Sicheng Wu
Donghua University - Songjiang Campus: Donghua University

Research Article

Keywords: NO, SO2, Hg0, Absorption, Micro-nanobubble, Urea

Posted Date: February 18th, 2021

DOI: https://doi.org/10.21203/rs.3.rs-159410/v1

Simultaneous Removal of NO, SO_2 and Hg^0 with the WDRMRS

Mingqiang Deng[1], Zhengguo Xiao [2 *], Dengxin Li [1, 3 *], Qiaoling Zhu [1], Qin Chen [1], Sicheng Wu [1]

[1] College of Environmental Science and Engineering, Donghua University, Shanghai, 201620, PR, China

[2] Shanghai Textile Research Institute Co. Ltd, Shanghai, 200082, PR, China

[3] State Key Laboratory of Pollution Control and Resource Reuse, College of Environmental Science and Engineering, Tongji University, Shanghai, 200092, PR, China

E-mail: mqdeng@126.com, 516338462@qq.com, lidengxin@dhu.edu.cn, a1085462316@163.com, chenqin@sspu.edu.cn, sichengwu18@163.com,

[*] **Corresponding author: Tel.: +86 18621587528, E-mail: 516338462@qq.com; Tel.: +86 13636641041, Fax: +86 21 67792522, E-mail: lidengxin@dhu.edu.cn**

Abstract

Micro-nanobubbles can spontaneously generate hydroxyl free radicals (·OH). Urea is a cheap reductant and can react with NOx species, and their products are nontoxic and harmless N_2, CO_2 and H_2O. In this study, a Wet Direct Recycling Micro-nanobubble Flue Gas Multi-pollutants Removal System (WDRMRS) was developed for the simultaneous removal of NO, SO_2 and Hg^0. In this system, a micro-nanobubble generator (MNBG) was used to produce a micro-nanobubble gas-liquid dispersion system (MNBGLS) through recycling the urea solution from the reactor and the simulated flue gas composed of N_2, NO, SO_2 and Hg^0. The MNBGLS, which has a large gas-liquid dispersion interface, was recycled continuously from the MNBG to the reactor, thus achieving cyclic absorption of various pollutants. All of the investigated parameters, including the initial pH and temperature of the absorbent as well as the concentrations of urea, NO and SO_2 had significant effects on the NO removal efficiency but did not significantly affect the SO_2 removal efficiency, whereas only

the initial solution pH and NO concentration affected the Hg^0 removal efficiency. The analysis results of the reaction mechanism showed that $\cdot OH$ played a critical role in the removal of various pollutants. After the treatment by this system, the main removal products were HgO sediment, SO_4^{2-} and NH^{4+} which could be easily recycled.

Keywords: NO; SO_2; Hg^0; Absorption; Micro-nanobubble; Urea

1. Introduction

Nitrogen oxides (NOx) and sulfur dioxide (SO_2), the major air pollutants, are the main precursors for acid rain and photochemical smog, and mercury (Hg), which is considered to be one of the most toxic heavy metals, has received increasing attention because it has persistence, bio-accumulation and neurological toxicity (Wei et al., 2009; Fang et al., 2011; Zheng et al., 2007; Rallo et al., 2012; Ye et al., 2014; Xie et al., 2013). NOx, SO_2 and Hg are the typical components in coal-fired flue gas. The Chinese government attaches great importance to air pollution control and takes effective measures to prevent and control NOx, SO_2 and Hg pollution from flue gas. At present, as a mature method for NOx, SO_2 and Hg removal in flue gas, the combined system of selective catalytic reduction (SCR) (Krishna and Makkee, 2005; Wu et al., 2008), wet flue gas desulfurization (WFGD) (Sharma et al., 2012) and activated carbon injection (ACI) (Rallo et al., 2012; Yang et al., 2007) has been widely applied. Although this system can achieve the deep removal of NOx, SO_2 and Hg^0, it still has some disadvantages such as the high cost of construction and operation, high occupational area, high complexity, low stability, ammonia leakage, and secondary pollution (Wang et al., 2019; Guo et al., 2012). Another method is an integrated removal process by which NOx, SO_2 and Hg^0 are simultaneously removed in the same device. This process can avoid the disadvantages of the aforementioned method, simplifying the system, reducing the cost, and still obtaining the high removal efficiency. The wet liquid phase oxidation-absorption process which can oxidize and absorb NOx, SO_2 and Hg^0 in one-step, is the main direction of the future research on the integrated removal of multi-pollutants from the flue gas (Wang et al., 2019).

As for the simultaneous removal of NOx, SO_2 and Hg^0, the key issue is to remove nitric oxide (NO) and Hg^0 efficiently and rapidly because NO, which is sparsely soluble in water, accounts for 90%~95% of NOx in flue gas (Zhao et al., 2016) and Hg^0 is insoluble in the water. According to the literature and our previous study, micro-nanobubbles (MNBs) can spontaneously generate a large amount of hydroxyl free radicals ($\cdot OH$) with a high oxidizing ability (Takahashi et al., 2007; Xiao et al., 2019b, 2020a), which can not only oxidize NO into NO_2 but oxidize Hg^0 into mercuric hydroxide or mercuric oxide, as shown in reaction (1) (Zhao et al., 2014a, 2014b; Liu and Wang, 2018). Liu et al. (2015) conducted the simultaneous removal of NO, SO_2 and Hg^0 by using a Fenton-like reagent based on Fe^{3+} in a spray reactor, and the results showed that $\cdot OH$ generated from the Fenton-like regent played a critical role in the removal of NO, SO_2 and Hg^0, and the removal efficiencies of NO, SO_2 and Hg^0 were 85.3%, 100% and 100%, respectively, under the optimal conditions. Urea $(NH_2)_2CO$), which is cheap, nontoxic, harmless and easy to obtain, is a strong reductant with weak alkalinity. Fang et al. (2011) found that urea could effectively promote the removal of NO_2, and the main reaction products are the recyclable ammonium sulfate and nontoxic and harmless gases (CO_2 and N_2). Therefore, urea is an economic and eco-friendly reagent for the removal of multi-pollutants from flue gas.

$$Hg^0 + 2 \cdot OH \rightarrow Hg(OH)_2 \overset{heat}{\rightarrow} HgO + H_2O \quad (1)$$

In this work, we developed a Wet Direct Recycling Micro-nanobubble Flue Gas Multi-pollutants Removal System (WDRMRS), in which a micro-nanobubble gas-liquid dispersion system (MNBGLS) was generated by utilizing a micro-nanobubble generator (MNBG) to inject the simulated flue gas consisting of N_2, NO, SO_2 and Hg^0 and recycle a urea aqueous solution of a certain concentration from a column reactor. The MNBGLS recycled continuously from the MNBG to the reactor. The continuous cyclic absorption of NO, SO_2 and Hg^0 was achieved through a series of oxidation-reduction reactions in the reactor. Moreover, the MNBGLS has a high gas-liquid dispersion interface and can enhance the gas solubility (Xiao et al., 2020a). To explore the performance of the oxidation-reduction system of the MNBGLS based on urea, the effects of the important operational parameters on the simultaneous removal of NO, SO_2 and Hg^0, such as initial pH and temperature of the absorbent, urea concentration, NO concentration and SO_2 concentration, were investigated.

2. Materials and methods

2.1. Materials and instruments

Materials and instruments are respectively provided in Tables 1 and 2 in Supplementary materials in Appendix A.

2.2. Experimental procedure

The experimental setup is shown in Fig. 1, and the detailed experimental procedures are described as follows.

First, urea aqueous solution (190 L) is prepared and fed into a column reactor (22) from the absorbent inlet (24) on the top of the reactor. To obtain the experimental requirements, a heating tube (26) and temperature controller (25) are used to adjust the solution temperature, and HCl and NaOH are used to adjust the solution pH. Then, the mixed solution (0.8 L), in which the concentrations of potassium permanganate and urea are 7 mmol/L and 5 wt.%, respectively, and the pH is 8, is prepared and fed into a three-neck flask (19). The digital display constant temperature water baths (8) and (18) are turned on and their temperature readings are set as 303 K and 328 K, respectively.

Second, the gas control valves (13) and (16) are opened, and the gas control valves (14), (15) and (17) are closed. The gas relief valves on the cylinders (1-3) are all opened so that NO, SO_2, and N_2 flow into a surge flask (10) by passing through the rotameters (4-6). Meanwhile, the carrier gas of Hg^0 and N_2 passes through a rotameter (7) (flow rate: 200 ml/min) to bring Hg^0 vapor from a mercury permeation tube (9) into the surge flask (10), thus forming the simulated flue gas, which flows into a flue gas analyzer (12), with which the concentrations of NO and SO_2 are measured by passing through a rotameter (11) (flow rate: 2 L/min). The excess gas is released after being absorbed in the tail gas absorption tank (20). The desired gas concentration is achieved by adjusting the gas flow.

Third, the gas control valves (13) and (16) are closed and the gas control valves (14), (15) and (17) are opened after the gas concentration stabilizes. Meanwhile, the MNBG (21) is turned on to simultaneously inhale the simulated flue gas from the surge flask (10) and the absorbent from the column reactor (22) to form the MNBGLS, which is injected back into the reactor again for recycling. The excess gas enters the three-neck flask (19) and is absorbed. Then, the absorbed tail gas is released after being absorbed again in the tail gas absorption tank (20). The concentration of the gas released from the reactor is measured with the flue gas analyzer (12).

Finally, the system is turned off after running for 60 min. The test sample is then collected from the absorbent outlet (23) at the bottom of the column reactor (22). After the end of every single experiment, the absorbed liquid is discharged from the absorbent outlet (23) into the waste liquid storage tank and treated as the waste liquid.

2.3. Analysis methods

2.3.1. NO/SO_2 removal efficiencies

The removal efficiencies of NO and SO_2 can be calculated as follows:

$$\eta = \frac{(C_{in} - C_{out})}{C_{in}} \times 100\%, \quad (2)$$

where η (%) represents the removal efficiency, C_{in} (ppm) represents inlet NO/SO_2 concentrations, and C_{out} (ppm) represents outlet NO/SO_2 concentrations.

2.3.2. Hg^0 removal efficiency

According to the results of Fang et al. (2013), under the conditions of 7 mmol/L potassium permanganate, 5 wt.% urea, 52.1 μg/m^3 Hg^0, 650 mg/m^3 NO, 2900 mg/m^3 SO_2, 7% O_2 and a solution temperature of 328 K, the Hg^0 removal efficiency was 100% when the solution was alkaline. Thus, five groups of experiments were

designed to test the absorption efficiency of 0.8 L of mixed solution of potassium permanganate and urea for Hg^0. ICP was used to test the concentration of Hg^0 in the absorbed solution, and the absorption efficiency of Hg^0 was calculated by formula (3):

$$E = \frac{150\times60-C_{Hg}\times v\times10^6}{150\times60}\times 100\% \quad (3)$$

where E (%) is the absorption efficiency of Hg^0, C_{Hg} (mg/L) is the concentration of Hg^0 in the absorbed solution, and v (L) is the volume of the absorbed solution. The detailed experimental conditions and results are provided in Table 3 which is showed in Supplementary materials in Appendix A.

Based on these experimental results, ICP is utilized to test the sample liquid from the column reactor and three-neck flask to determine the Hg^0 concentration before entering the reactor and after the removal reaction, respectively, and the Hg^0 removal efficiency is calculated by formula (4):

$$\eta' = \frac{C'_{in}\times V_1-C'_{out}\times V_2}{C'_{in}\times V_1}\times 100\% \quad (4)$$

where η' (%) is the Hg^0 removal efficiency, C'_{in} (mg/L) is the concentration of Hg^0 in the three-neck flask, V_1 (L) is the volume of the solution in the three-neck flask, C'_{out} (mg/L) is the concentration of Hg^0 in the column reactor, and V_2 (L) is the volume of the solution in the column reactor.

2.3.3. Detection of the reaction products

NO_2^-, NO_3^-, SO_3^{2-}, and SO_4^{2-} in the reaction products are detected by IC (ICS-1000), and NH_4^+ in the reaction products is detected by IC (DX-600).

3. Results and discussion

3.1. Effects of the urea concentration

As shown in Fig. 2, the urea concentration had little effect on the removal efficiencies of SO_2 and Hg^0. No matter whether urea was added or not, the SO_2 removal efficiency was greater than 99.6% and the Hg^0 removal efficiency was maintained at approximately 86%. However, the urea concentration significantly affected the NO removal efficiency, which first increased and then slightly decreased as the urea concentration increased. This was because the chemical reactivity and physical properties of urea caused changes in the NO removal efficiency. On the one hand, urea could react with the main N species in the solution including NO, NO_2, NO_2^-, and NO_3^-, thus accelerating the oxidation and absorption of NO and promoting NO removal. On the other hand, with the increase in the urea concentration, the viscosity of the absorption solution increased so that the diffusion rate and solubility of NO in the liquid phase decreased (Wei et al., 2009), thus inhibiting the oxidation and absorption of NO. Therefore, the NO removal efficiency decreased when the urea concentration increased from 3 g/L to 5 g/L. To obtain the best removal effects, the urea concentration was designed as 3 g/L in subsequent experiments.

3.2. Effects of the initial solution pH

The effects of various initial solution pH values (3.47, 5.51, 7.46, 9.46 and 10.47) on the removal efficiencies of NO, SO_2 and Hg^0 were investigated (Fig. 3). With the increase in the initial pH of urea solution, the SO_2 removal efficiency did not change significantly but only increased slightly from 99.4% to 99.9%. Meanwhile, the NO removal efficiency increased first and then decreased, and it reached the highest value (96.7%) at pH=9.46, which was, however, only 0.6 higher than that at a pH=7.46 (the original pH of the 3 g/L urea solution). Moreover, the Hg^0 removal efficiency decreased slightly as the pH increased. Therefore, to give consideration to the removal effects and convenience of the system operation, the initial solution pH of the subsequent experiments was designed to be 7.46.

According to the relevant literature, under strong acidic conditions, the presence of a great deal of H^+ was not conducive to the reaction of $\cdot OH$ and NO (Xiao et al., 2019a), and it also accelerated the decomposition of HNO2 so that NO was regenerated in the removal reaction (Fang et al., 2011), thus inhibiting NO removal. Hence, as shown in reaction (1), more $\cdot OH$ participated in the reaction of Hg^0 so that the removal efficiency of

Hg^0 increased. However, the weak acidic conditions were conducive to the hydrolysis of urea, which could promote the oxidation and absorption of NO (Fang et al., 2013). Moreover, with the increase in the solution pH, more and more OH^- could absorb H^+ through the acid-base neutralization reaction (5) to promote the oxidation of $\cdot OH$ to NO (Liu et al., 2010; Guo et al., 2018), thus improving the NO removal efficiency. Some researchers indicated that OH^- could consume $\cdot OH$ via reaction (6) at a very high rate ($1.3\times1010\ M^{-1}s^{-1}$) (Liu and Wang, 2017; Lau et al., 2011; Liu et al., 2014), and radical ions ($\cdot O^-$) reacted more slowly with the same substrate than $\cdot OH$ (Adewuyi and Appaw, 2002); therefore, too high of a solution pH weakened the oxidation capacity of the MNBGLS, resulting in the inhibition of NO removal. In addition, the MNBs could not only grow in size but collapse faster because the excessive OH^- repelled OH^- on the surface of the MNBs to aggravate the movement of bubbles, thus decreasing the retention time of the bubbles in the water (Bunkin et al., 2012) and further inhibiting the absorption of NO. Therefore, the NO removal efficiency decreased when the initial solution pH increased from 9.46 to 10.47. Meanwhile, due to the competition between the reaction of $\cdot OH$ and NO and the reaction of $\cdot OH$ and Hg^0, the Hg^0 removal efficiency decreased as the solution pH increased.

$$OH^- + H^+ \rightarrow H_2O \quad (5)$$

$$\cdot OH + OH^- \rightarrow H_2O + \cdot O^- \quad (6)$$

3.3. Effects of the initial solution temperature

As shown in Fig. 4, with the increase in the initial solution temperature, the removal efficiencies of SO_2 and Hg^0 were insignificantly affected, but the NO removal efficiency gradually decreased, indicating that this MNBGLS based on urea had good performance in the removal of NO, SO_2 and Hg^0 under normal temperature conditions. According to the research, an increase in the solution temperature had four effects: the hydrolysis of urea was promoted to improve the oxidation and absorption of NO (Fang et al., 2013); the active molecules in the solution increased and their reactivity was enhanced, thus increasing the reaction rate (Glassman et al., 2015); the gas solubility decreased (Liu and Wang, 2017; Liu et al., 2018); and the stability of the MNBs

declined, which further affected the gas solubility (Luo et al., 2009; Temesgen et al., 2017). Amongst these effects, the former two effects promoted NO removal, while the latter two effects inhibited NO removal. In this work, due to the dominant inhibitory effect, the NO removal efficiency decreased as the solution temperature increased.

3.4. Effects of the NO concentration

As shown in Fig. 5, with the increase in the NO concentration, the SO_2 removal efficiency changed insignificantly, while the removal efficiencies of NO and Hg^0 gradually decreased. It is worth noting that the performance of the MNBGLS remained unchanged because of the rated inlet gas flow and recycling solution volume of the MNBG. Therefore, more $\cdot OH$ generated from the MNBs participated in the oxidation and absorption of NO due to the less NO entering the reactor under low NO concentrations. As the NO concentration increased, the quantities of NO molecules entering the reactor per unit time raised to increase the gas to liquid relative molar ratio of NO and solution (Liu and Zhang, 2011) so that NO was released more easily because more NO was not oxidized in time. Additionally, since the reaction of $\cdot OH$ and NO competed with the reaction of $\cdot OH$ and Hg^0, more NO entered the system to consume more $\cdot OH$, resulting in less $\cdot OH$ involved in the oxidation reaction of Hg^0. Consequently, increasing the NO concentration decreased the removal efficiencies of NO and Hg^0.

3.5. Effects of the SO_2 concentration

The effects of the SO_2 concentration on the simultaneous removal efficiencies of NO, SO_2 and Hg^0 were also investigated (Fig. 6). Due to the high solubility of SO_2, the removal efficiencies of SO_2 and Hg^0 were not affected by the changes in the SO_2 concentration and were maintained above 99.8% and at approximately 86%, respectively. Nevertheless, the increase in the SO_2 concentration had a significant effect on the NO removal efficiency. The NO removal efficiency increased sharply from 85% to 92.9% when the SO_2 concentration

increased from 0 to 950 ppm and then slowly increased as the SO_2 concentration increased from 950 ppm to 2750 ppm, but it declined significantly when the SO_2 concentration increased from 2750 ppm to 3550 ppm. The reasons could be explained as follows: SO_2 entered the liquid phase and was quickly dissolved into the water to form HSO_3^- and SO_3^{2-} (Colle et al., 2004, 2005), both of which reacted with NO, NO_2, NO_2^- and NO_3^- to promote the oxidation and absorption of NO (Takeuchi et al., 1977; Weisweiler and Blumhqfer, 1984). Moreover, HSO_3^- and SO_3^{2-} could also combine with NO to form $(ONSO_3)^{2-}$, which further improved the absorption of NO (Littlejohn, 1986). Hence, the NO removal efficiency increased as the SO_2 concentration increased. However, HSO_3^- and SO_3^{2-} were also the scavengers of $\cdot OH$, thus consuming more $\cdot OH$ as the SO_2 concentration increased and inhibiting the removal of NO. When the SO_2 concentration rose from 2750 ppm to 3550 ppm, this inhibition played a leading role in the removal of NO, causing the decrease of the NO removal efficiency. In the system, the NO removal efficiency in the presence of SO_2 is generally higher than that in the absence of SO_2.

3.6. Parallel tests

Parallel tests were conducted under the optimal conditions (3 g/L urea concentration, initial solution pH of 7.46, initial solution temperature of 298 K, 750 ppm NO, 2750 ppm SO_2, and a Hg^0 penetration rate of 150 ng/min). As shown in Table 1, the removal efficiencies of NO, SO_2 and Hg^0 exhibited good reproducibility, indicating that the system had stable performance and could provide a reference for its industrial application.

Table 1 Results of parallel tests

Removal efficiency (%)	Experimental groups			Average removal efficiency (%)	Standard deviation
	1	2	3		
NO	97.6	97.1	97.7	97.5	0.3528
SO_2	99.7	99.9	99.8	99.8	0.1091
Hg^0	87.7	86.8	87.1	87.2	0.4583

3.7. Reaction mechanism

Table 2 shows the detection of the reaction products.

Table 2 Products in the absorption solution

Ions	NH^{4+}	NO_3^-	NO_2^-	SO_4^{2-}	SO_3^{2-}
Concentration (mg/L)	0.15	0.04	—	1.59	—

As shown in Table 2, NO_2^- and SO_3^{2-} were not detected, and the reaction products were mainly SO_4^{2-} and NH^{4+}, with only a small amount of NO_3^-. This was because the reaction between nitrous acid and urea was stronger than that between nitric acid and urea (Fang et al., 2011), and nitric acid was relatively steady in the solution. SO_3^{2-} could not only be oxidized by $\cdot OH$ to SO_4^{2-} but also participated in the oxidation-absorption of NO, thus being consumed. NH^{4+} was produced by the hydrolysis of urea.

The chemical reactions of NO, SO_2 and Hg^0 in this system are complicated, but the main reaction mechanisms can be inferred from the results in Table 2 and are depicted in Fig. 7. When the MNBs collapse in the MNBGLS, $\cdot OH$ is generated and NO, SO_2 and Hg^0 are also released from the bubbles. SO_2 quickly dissolves into the water and is converted to HSO_3^-, SO_3^{2-} and H^+ (reactions (7) and (8)) (Xiao et al., 2020b). Part of the SO_2 in the gas phase is also oxidized by $\cdot OH$ to SO_4^{2-} (reactions (9) and (10)) (Wu et al., 2018).

$$SO_2 + H_2O \leftrightarrow HSO_3^- + H^+ \quad (7)$$

$$HSO_3^- \leftrightarrow SO_3^{2-} + H^+ \quad (8)$$

$$SO_2 + \cdot OH \rightarrow HSO_3 \quad (9)$$

$$HSO_3 + \cdot OH \rightarrow 2H^+ + SO_4^{2-} \quad (10)$$

NO is oxidized by $\cdot OH$ and absorbed in the water to form NO_3^- and NO_2^- (reactions (11-16)) (Xiao et al., 2019a). Additionally, NO can also combine with NO_2 to form N_2O_3, and NO_2 and N_2O_4 can convert into each other. In the liquid phase, the highly soluble compounds N_2O_3 and N_2O_4 also dissolve and react rapidly with

water to produce equimolar amounts of HNO_2 and HNO_3 (Fang et al., 2011). Therefore, the main NOx species in the gas and liquid phases may be NO, NO_2, N_2O_3, N_2O_4, HNO_2 and HNO_3.

$$NO + \cdot OH \rightarrow H^+ + NO_2^- \quad (11)$$

$$NO + \cdot OH \rightarrow NO_2 + \cdot H \quad (12)$$

$$NO_2 + \cdot OH \rightarrow H^+ + NO_3^- \quad (13)$$

$$NO_2^- + \cdot OH \rightarrow NO_3^- + \cdot H \quad (14)$$

$$2NO_2 + H_2O \rightarrow 2H^+ + NO_3^- + NO_2^- \quad (15)$$

$$3HNO_2 \rightarrow 2NO + H^+ + NO_3^- + H_2O \quad (16)$$

Urea in the MNBGLS hydrolyzes to produce ammonium carbamate (NH_2COONH_4) (reaction 17). Urea can react with NO and NO_2, NH_2COONH_4 can react with HNO_2 and HNO_3, and all of these reactions produce N_2 and CO_2 (reactions (18-21)) (Fang et al., 2011, 2013).

$$(NH_2)_2CO + H_2O \leftrightarrow NH_2COONH_4 \quad (17)$$

$$2(NH_2)_2CO + 6NO \rightarrow 5N_2 \uparrow + 2CO_2 \uparrow + 4H_2O \quad (18)$$

$$4(NH_2)_2CO + 6NO_2 \rightarrow 7N_2 \uparrow + 4CO_2 \uparrow + 8H_2O \quad (19)$$

$$6NO_3^- + 6H^+ + 5NH_2COONH_4 \rightarrow 8N_2 \uparrow + 5CO_2 \uparrow + 13H_2O \quad (20)$$

$$2NO_2^- + 2H^+ + NH_2COONH_4 \rightarrow 2N_2 \uparrow + CO_2 \uparrow + 3H_2O \quad (21)$$

In addition, HSO_3^- and SO_3^{2-}, formed through SO_2 dissolving in the water, are also involved in the reaction of NOx (reactions (22-29)) (Takeuchi et al., 1977; Weisweiler and Blumhqfer, 1984; Littlejohn et al., 1993; Clifton et al., 1988; Shen and Rochelle, 1998; Xiong et al., 2018), but reaction (26) did not occur easily under the alkaline conditions (Xiong et al., 2018). During the removal reaction, HSO_3^- and $SO_3^{2-}$are also oxidized by $\cdot OH$ to SO_4^{2-} (reactions (30-32)) (Wu et al., 2018; Tokunaga and Suzuki, 1984; Gerasimov et al., 1996; Mok and Namb, 2002) so that no SO_3^{2-} was detected in the reaction products.

$$2NO_2 + H_2O + SO_3^{2-} \rightarrow 2H^+ + 2NO_2^- + SO_4^{2-} \quad (22)$$

$$2NO_2 + H_2O + 2SO_3^{2-} \rightarrow 2HSO_3^- + NO_2^- + NO_3^- \quad (23)$$

$$NO_2 + H_2O + HSO_3^- \rightarrow 3H^+ + 2NO_2^- + SO_4^{2-} \quad (24)$$

$$4SO_3^{2-} + 2NO_2^- \rightarrow N_2 + 4SO_4^{2-} \quad (25)$$

$$3SO_3^{2-} + 2NO_3^- + 2H^+ \rightarrow 2NO + 3SO_4^{2-} + OH^- \quad (26)$$

$$2NO + 2SO_3^{2-} \leftrightarrow N_2 + 2SO_4^{2-} \quad (27)$$

$$2NO + HSO_3^- \leftrightarrow N_2O + SO_4^{2-} + H^+ \quad (28)$$

$$5N_2O + H_2O \rightarrow 2H^+ + 2NO_3^- + 4N_2 \quad (29)$$

$$HSO_3^- + \cdot OH \rightarrow \cdot SO_3^- + H_2O \quad (30)$$

$$SO_3^{2-} + \cdot OH \rightarrow \cdot SO_3^- + OH^- \quad (31)$$

$$\cdot SO_3^- + \cdot OH \rightarrow SO_4^{2-} + \cdot H \quad (32)$$

With regard to Hg^0, it is oxidized by $\cdot OH$ to $Hg(OH)_2$ (reaction (1)), which is easily heated to produce HgO sediment, thus achieving the removal of Hg^0.

4. Conclusions

The recycling oxidation-reduction process of MNBGLS based on urea, which was proposed in this study, succeeded in simultaneously removing NO, SO_2 and Hg^0. Under the optimal conditions, the average removal efficiencies of NO, SO_2 and Hg^0 were 97.5%, 99.8% and 87.2%, respectively. Increasing solution temperature and NO concentration decreased the removal efficiencies of NO and Hg^0, whereas with the increase in solution pH and concentrations of urea and SO_2, Hg^0 removal efficiency did not change obviously but NO removal efficiency increased firstly and then decreased. All of the investigated parameters had an insignificant effect on SO_2 removal efficiency. The reaction mechanism was deduced according to the analysis of the removed products and it was found that the oxidation of $\cdot OH$ generated from the MNBs played a dominant role in the removal of NO, SO_2 and Hg^0, meanwhile urea further promoted the removal of NO through reduction reaction. The main removal products were SO_4^{2-}, NH^{4+}, a small amount of NO_3^-, as well as non-toxic and harmless N_2. N_2 can be directly discharged and other removal products can be made into nitrogen fertilizer after Hg^{2+} in them is separated by heating, so as to improve the economic benefits of flue gas treatment and reduce the treatment costs.

Acknowledgments

This work was supported by the Iron and Steel Joint Research Fund of National Natural Science Foundation-China BaoWu Steel Group Co., Ltd. (No. U1660107) and the Fundamental Research Funds for the Central Universities and the Graduate Student Innovation Fund of Donghua University (No. CUSF-DH-D-2019077). The authors also appreciate the support from the Shanghai Municipal Bureau of Ecology and Environment, People's Republic of China.

Ethics declarations

Ethical approval

No ethical approval was necessary for this study.

Consent to participate

All participants in this study consent to participation.

Consent to publish

All authors consent to this publication.

Competing Interests

The authors declare that they have no known competing interests.

Authors Contributions

Mingqiang Deng conducted the experiment, analyzed, interpreted data, and helped writing the manuscript. Zhengguo Xiao helped writing and revising the manuscript. Dengxin Li supervised the research and searched funding for the project. Qiaoling Zhu organized figures and tables, helped writing and revising the manuscript. Qin Chen interpreted data, helped revising the manuscript. Sicheng Wu organized figures and tables.

Availability of data and materials

The datasets and materials used and/or analyzed during the current study are available from the author and corresponding author on reasonable request.

Appendix A. Supplementary materials

References

Adewuyi, Y.G., Appaw, C., 2002. Sonochemical oxidation of carbon disulfide in aqueous solutions: reaction kinetics and pathways. Ind. Eng. Chem. Res. 41, 4957－4964.

Bunkin, N.F., Yurchenko, S.O., Suyazov, N.V., Shkirin, A.V., 2012. Structure of the nanobubble clusters of dissolved air in liquid media. J. Biol. Phys. 38, 121－152.

Clifton, C.L., Altstein, N., Huie, R.E., 1988. Rate constant for the reaction of nitrogen dioxide with sulfur(IV) over the pH range 5.3-13. Environ. Sci. Technol. 22, 586－589.

Colle, S., Vanderschuren, J., Thomas, D., 2004. Pilot-scale validation of the kinetics of SO_2 absorption into sulphuric acid solutions containing hydrogen peroxide. Chem. Eng. Process. 43, 1397－1402.

Colle, S., Vanderschuren, J., Thomas, D., 2005. Simulation of SO_2 absorption into sulfuric acid solutions containing hydrogen peroxide in the fast and moderately fast kinetic regimes. Chem. Eng. Sci. 60, 6472－6479.

Fang, P., Cen C.P., Tang, Z.X., Zhong, P.Y., Chen, D.S., Chen, Z.H., 2011. Simultaneous removal of SO_2 and NOx by wet scrubbing using urea solution. Chem. Eng. J. 168, 52－59.

Fang, P., Cen, C.P., Wang, X.M., Tang, Z.J., Tang, Z.X., Chen, D.S., 2013. Simultaneous removal of SO_2, NO and Hg^0 by wet scrubbing using urea + $KMnO_4$ solution. Fuel Process. Technol. 106, 645－653.

Glassman, I., Yetter, R.A., Glumac, N.G., 2015. Chapter 2-Chemical kinetics combustion. fifth edition, Elsevier, Amsterdam, 41－70.

Guo, L.F., Shu, Y.J., Gao, J.M., 2012. Present and future development of flue gas control technology of DeNO_X in the world. Energ. Procedia 17, 397－403.

Gerasimov, G.Y., Gerasimova, T.S., Makarov, V.N., Fadeev, S.A., 1996. Homogeneous and heterogeneous radiation induced NO and SO_2 removal from power plants flue gases-modeling study. Radiat. Phys. Chem. 6, 763－769.

Guo, L.N., Han, C.Y., Zhang, S.L., Zhong, Q., Ding, J., Zhang, B.Q., Zeng, Y.Q., 2018. Enhancement effects of $\cdot O_2^-$ and ·OH radicals on NOx removal in the presence of SO_2 by using an O_3/H_2O_2 AOP system with inadequate O_3 (O_3/NO molar ratio = 0.5). Fuel 233, 769－777.

Krishna, K., Makkee, M., 2005. Coke formation over zeolite and CeO_2-zeolite and its influence on selective catalytic reduction of NOx. Appl. Catal. B: Environ. 62, 35－44.

Lau, L.C., Lee, K.T., Mohamed, A.R., 2011. Simultaneous SO_2 and NO removal using sorbents derived from rice husks: An optimisation study. Fuel 90, 1811－1817.

Liu, Y.X., Zhang, J., Sheng, C.D., Zhang, Y.C., Zhao, L., 2010. Simultaneous removal of NO and SO_2 from coal-fired flue gas by UV/H_2O_2 advanced oxidation process. Chem. Eng. J. 162, 1006－1011.

Liu, Y.X., Zhang, J., 2011. Photochemical oxidation removal of NO and SO_2 from simulated flue gas of coal-fired power plants by wet scrubbing using UV/H_2O_2 advanced oxidation process. Ind. Eng. Chem. Res. 50, 3836－3841.

Liu, Y.X., Pan, J.F., Zhang, J., 2014. Photochemical oxidation removal of Hg^0 from flue gas containing SO_2/NO by UV(ultraviolet)/H_2O_2 process. Energ. Fuel 28, 2135－2143.

Liu, Y.X., Zhou, J.F., Zhang, Y.C., Pan, J.F., Wang, Q., Zhang, J., 2015. Removal of Hg^0 and simultaneous removal of Hg^0/SO_2/NO in flue gas using two Fenton-like reagents in a spray reactor. Fuel 145, 180－188.

Liu, Y.X., Wang, Y., 2017. Simultaneous removal of NO and SO_2 using aqueous peroxymonosulfate with coactivation of Cu^{2+}/Fe^{3+} and high temperature. AIChE J. 63, 1287－1302.

Liu, Y.X., Wang, Y., 2018. Elemental mercury removal from flue gas using heat and Co^{2+}/Fe^{2+} coactivated oxone oxidation system. Chem. Eng. J. 348, 464－475.

Liu, Y.X., Liu, Z.Y., Wang, Y., Yin, Y.S., Pan, J.F., Zhang, J., Wang, Q., 2018. Simultaneous absorption of SO_2 and NO from flue gas using ultrasound/Fe^{2+}/heat coactivated persulfate system. J. Hazard. Mater. 342, 326－334.

Littlejohn, D., 1986. Kinetics of the reaction of nitric oxide with sulfite and bisulfate ions in aqueous solution. Inorg. Chem. 25, 3131－3185.

Littlejohn, D., Wang, Y.Z., Chang, S.G., 1993. Oxidation of aqueous sulfite ion by nitrogen dioxide. Environ. Sci. Technol. 27, 2162－2167.

Luo, J.H., Li, J., Huang, P., 2009. Huang M.Y. Kinetic rate constant of liquid drainage from colloidal gas aphrons. Chin. J. Chem. Eng. 17, 955－959.

Mok, Y.S., Namb, I.S., 2002. Modeling of pulsed corona discharge process for the removal of nitric oxide and sulfur dioxide. Chem. Eng. J. 85, 87－97.

Rallo, M., López-Antón, M.A., Contreras, M.L., Maroto-Valer, M.M., 2012. Mercury policy and regulations for coal-fired power plants. Environ. Sci. Pollut. Res. 19, 1084－1096.

Sharma, V.K., Sohn, M., Anquandah, G.A.K., Nesnas, N., 2012. Kinetics of the oxidation of sucralose and related carbohydrates by ferrate(VI). Chemosphere 87, 644－648.

Shen, C.H., Rochelle, G.T., 1998. Nitrogen dioxide absorption and sulfite oxidation in aqueous sulfite. Environ. Sci. Technol. 32, 1994－2003.

Takahashi, M., Chiba, K., Li, P., 2007. Free-radical generation from collapsing microbubbles in the absence of a dynamic stimulus. J. Phys. Chem. B 111, 1343－1347.

Takeuchi, H., Ando, M., Kizawa, N., 1977. Absorption of nitrogen oxides in aqueous sodium sulfite and bisulfite solutions. Ind. Eng. Chem. Process Des. Dev. 16, 303－308.

Temesgen, T., Bui, T.T., Han, M., Kim, T., Park, H., 2017. Micro and nanobubble technologies as a new horizon for water-treatment techniques: A review. Adv. Colloid Interfac. 246, 40－51.

Tokunaga, O., Suzuki, N., 1984. Radiation chemical reactions in NOx and SO_2 removals from flue gas. Radiat. Phys. Chem. 1, 145－165.

Wang, H., Yuan, B., Hao, R.L., Zhao, Y., Wang, X.P., 2019. A critical review on the method of simultaneous removal of multi-air-pollutant in flue gas. Chem. Eng. J. 378, 122155.

Wei, Z.S., Lin, Z.H., Niu, H.J.Y., He, H.M., Ji, Y.F., 2009. Simultaneous desulfurization and denitrification by microwave reactor with ammonium bicarbonate and zeolite. J. Hazard. Mater. 162, 837－841.

Wei, J.C., Luo, Y.B., Yu, P., Cai, B., Tan, H.Z., 2009. Removal of NO from flue gas by wet scrubbing with $NaClO_2/(NH_2)_2CO$ solutions. J. Ind. Eng. Chem. 15, 16－22.

Weisweiler, W., Blumhqfer, R., 1984. Absorption of NOx in aqueous solutions of $Na_2SO_3/NaHSO_3$ and simultaneous absorption of NOx and SOx in NaOH. Chem. Eng. 7, 241－247.

Wu, Z.B., Jiang, B.Q., Liu, Y., 2008. Effect of transition metals addition on the catalyst of manganese/titania for low-temperature selective catalytic reduction of nitric oxide with ammonia. Appl. Catal. B: Environ. 79, 347－355.

Wu, B., Xiong, Y.Q., Ge, Y.Y., 2018. Simultaneous removal of SO_2 and NO from flue gas with ·OH from the catalytic decomposition of gas-phase H_2O_2 over solid-phase $Fe_2(SO_4)_3$. Chem. Eng. J. 331, 343－354.

Xiao, Z.G., Aftab, T.B., Yuan, X.L., Xia, H.L., Li, D.X., 2019a. Experimental results of NO removal by the MBGLS. Micro Nano Lett. 14, 721－726.

Xiao, Z.G., Li, D.X., Zhang, R.L., Wang, F.K., Pan, F.F., Sun, Z.H., 2019b. An experimental study on the simultaneous removal of NO and SO_2 with a new wet recycling process based on the micro-nano bubble water system. Environ. Sci. Pollut. Res. 27, 4197－4205.

Xiao, Z.G., Li, D.X., Zhu, Q.L., Sun, Z.H., 2020a. Simultaneous removal of NO and SO_2 through a new wet recycling oxidation–reduction process utilizing micro-nano bubble gas–liquid dispersion system based on Na_2SO_3. Fuel 263, 116682.

Xiao, Z.G., Li, D.X., Wang, F.K., Sun, Z.H., Lin, Z.Y., 2020b. Simultaneous removal of NO and SO_2 with a new recycling micro-nano bubble oxidation-absorption process based on HA-Na. Sep. Purif. Technol. 242, 116788.

Xie, J.K., Qu, Z., Yan, N.Q., Yang, S.J., Chen, W.M., Hu, L.G., Huang, W.J., Liu, P., 2013. Novel regenerable sorbent based on Zr-Mn binary metal oxides for flue gas mercury retention and recovery. J. Hazard. Mater. 261, 206－213.

Xiong, Y.H., Zeng, Y.Q., Cai, W., Zhang, S.L., Ding, J., Zhong, Q., 2018. Experimental study on reaction characteristics of NO in $(NH_4)_2SO_3$ solution. J. Ind. Eng. Chem. 65, 380－386.

Yang, H.Q., Xu, Z.H., Fan, M.H., Bland, A.E., Judkins, R.R., 2007. Adsorbents for capturing Hg^0 in coal-fired boiler flue gas. J. Hazard. Mater. 146, 1－11.

Ye, J.H., Shang, J., Li, Q., Xu, W.W., Liu, J., Feng, X., Zhu, T., 2014. The use of vacuum ultraviolet irradiation to oxidize SO_2 and NOx for simultaneous desulfurization and denitrification. J. Hazard. Mater. 271, 89－97.

Zhao, Y., Hao, R.L., Guo, Q., 2014a. A novel pre-oxidation method for elemental mercury removal utilizing a complex vaporized absorbent. J. Hazard. Mater. 15, 118－126.

Zhao, Y., Hao, R.L., Zhang, P., Zhou, S.H., 2014b. An integrative process for Hg^0 removal using vaporized $H_2O_2/Na_2S_2O_8$. Fuel 136, 113－121.

Zhao, Y., Hao, R.L., Yuan, B., Jiang, J.J., 2016. Simultaneous removal of SO_2, NO and Hg^0 through an integrative process utilizing a cost-effective complex oxidant. J. Hazard. Mater. 301, 74－83.

Zheng, L.G., Liu, G.J., Chou, C.L., 2007. The distribution, occurrence and environmental effect of mercury in Chinese coals. Sci. Total Environ. 384, 374－383.

Figures

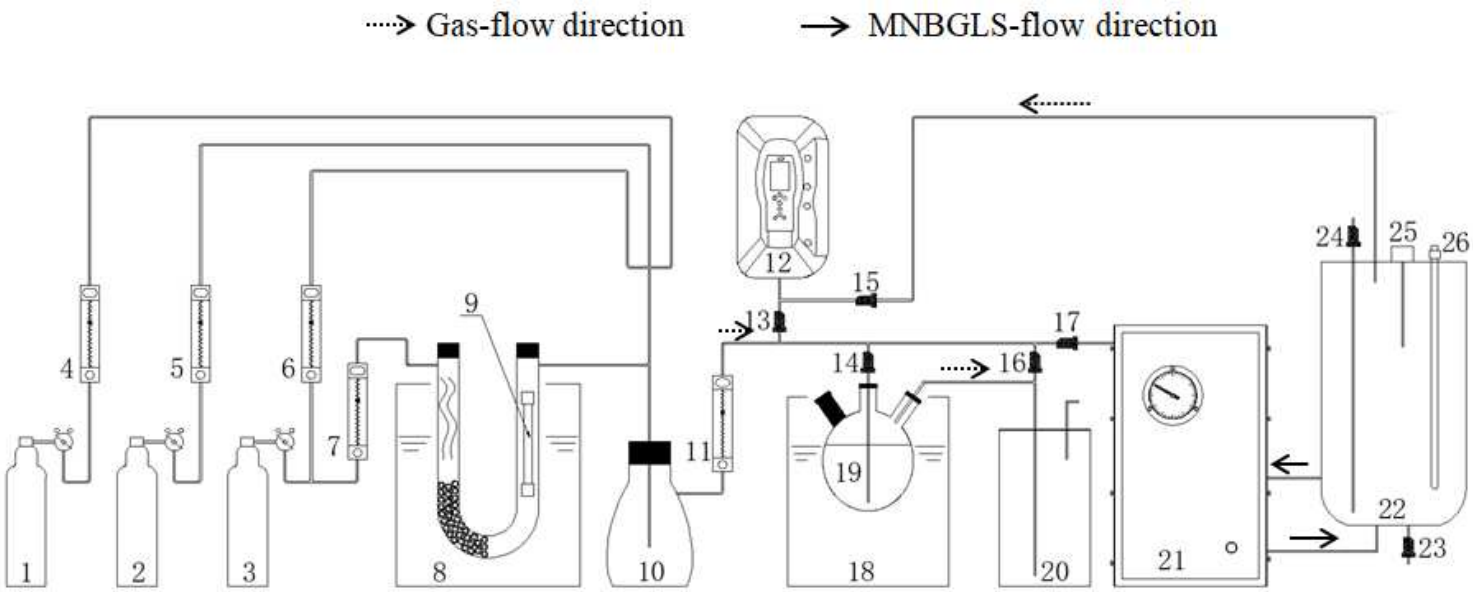

Figure 1

Schematic diagram of the experimental setup. 1. NO cylinder; 2. SO2 cylinder; 3. N2 cylinder; 4-7, 11. rotameter; 8, 18. digital display constant temperature water bath; 9. mercury penetration tube; 10. surge flask; 12. flue gas analyzer; 13-17. gas control valve; 19. three-neck flask; 20. tail gas absorption tank; 21. MNBG; 22. column reactor; 23. absorbent outlet with control valve; 24. absorbent inlet with control valve; 25. temperature controller; 26. heating tube.

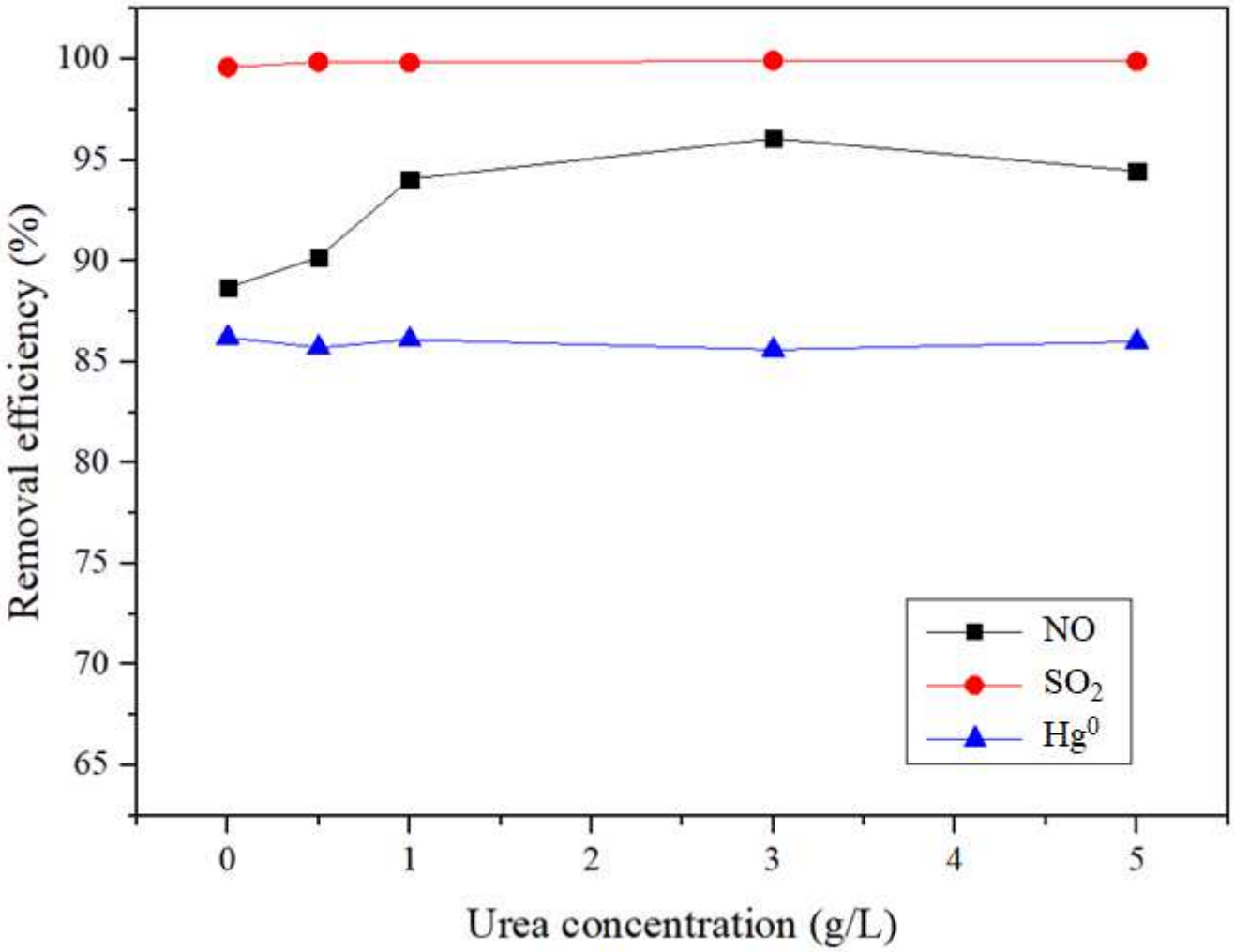

Figure 2

Effects of the urea concentration on the simultaneous removal efficiencies of NO, SO2 and Hg0. Experimental conditions: initial solution pH, 7.46; initial solution temperature, 298 K; 1750 ppm NO; 2750 ppm SO2; and Hg0 penetration rate, 150 ng/min.

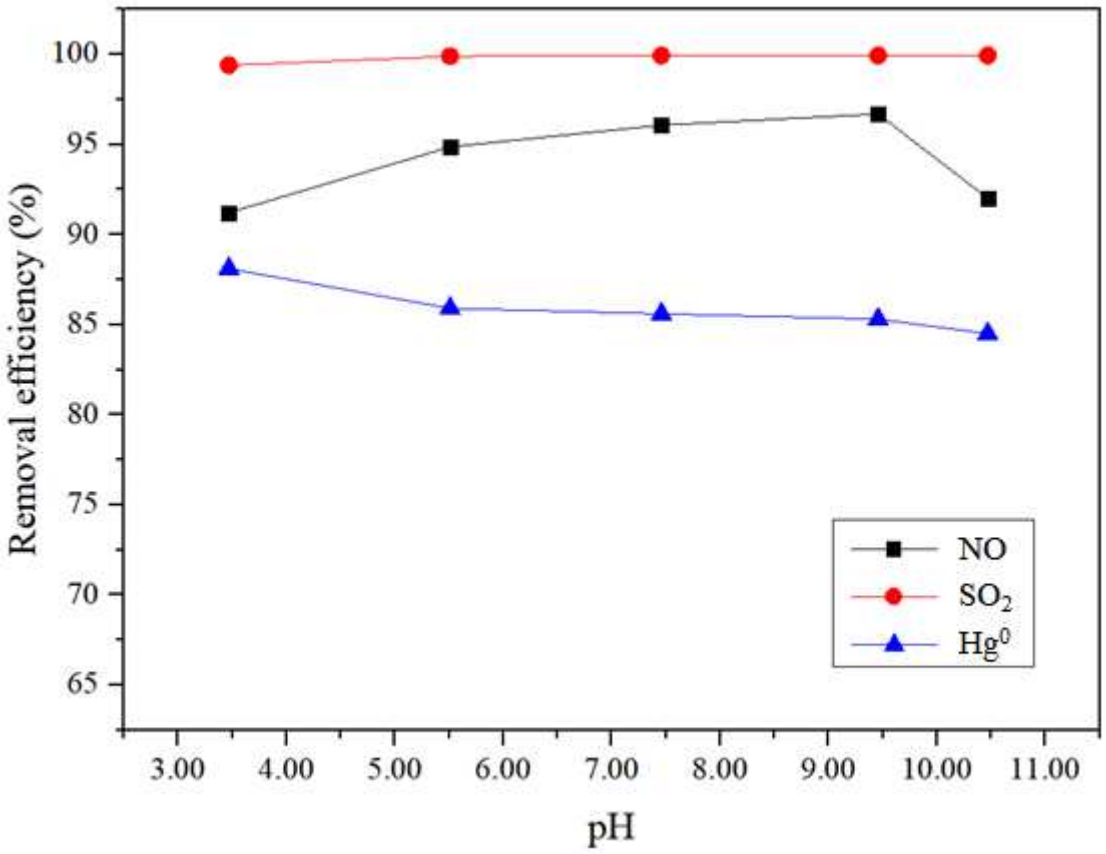

Figure 3

Effects of the initial solution pH on the simultaneous removal efficiencies of NO, SO2 and Hg0. Experimental conditions: 3 g/L urea; initial solution temperature, 298 K; 1750 ppm NO; 2750 ppm SO2; and Hg0 penetration rate, 150 ng/min.

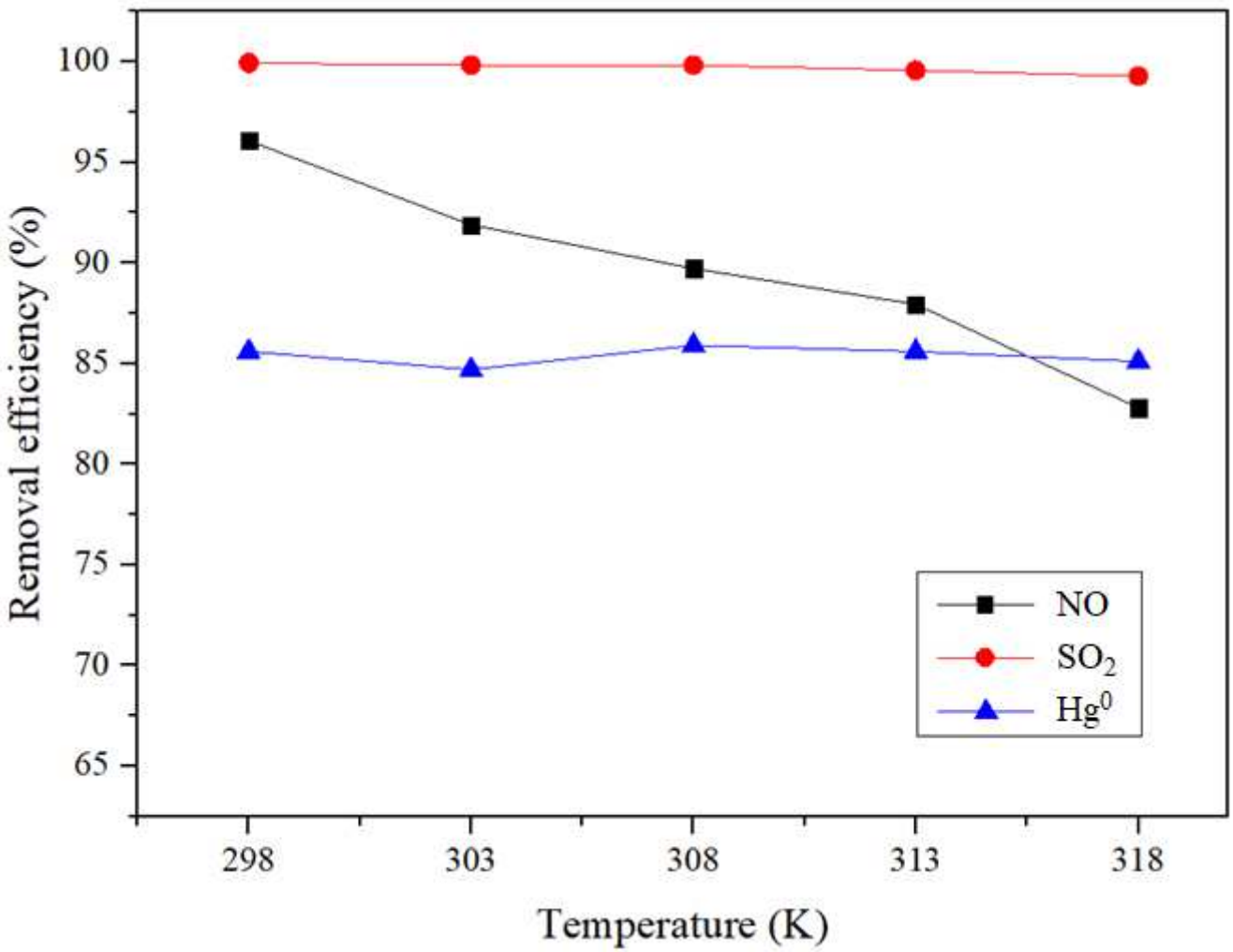

Figure 4

Effects of the initial solution temperature on the simultaneous removal efficiencies of NO, SO2 and Hg0. Experimental conditions: 3 g/L urea; initial solution pH, 7.46; 1750 ppm NO; 2750 ppm SO2; and Hg0 penetration rate, 150 ng/min.

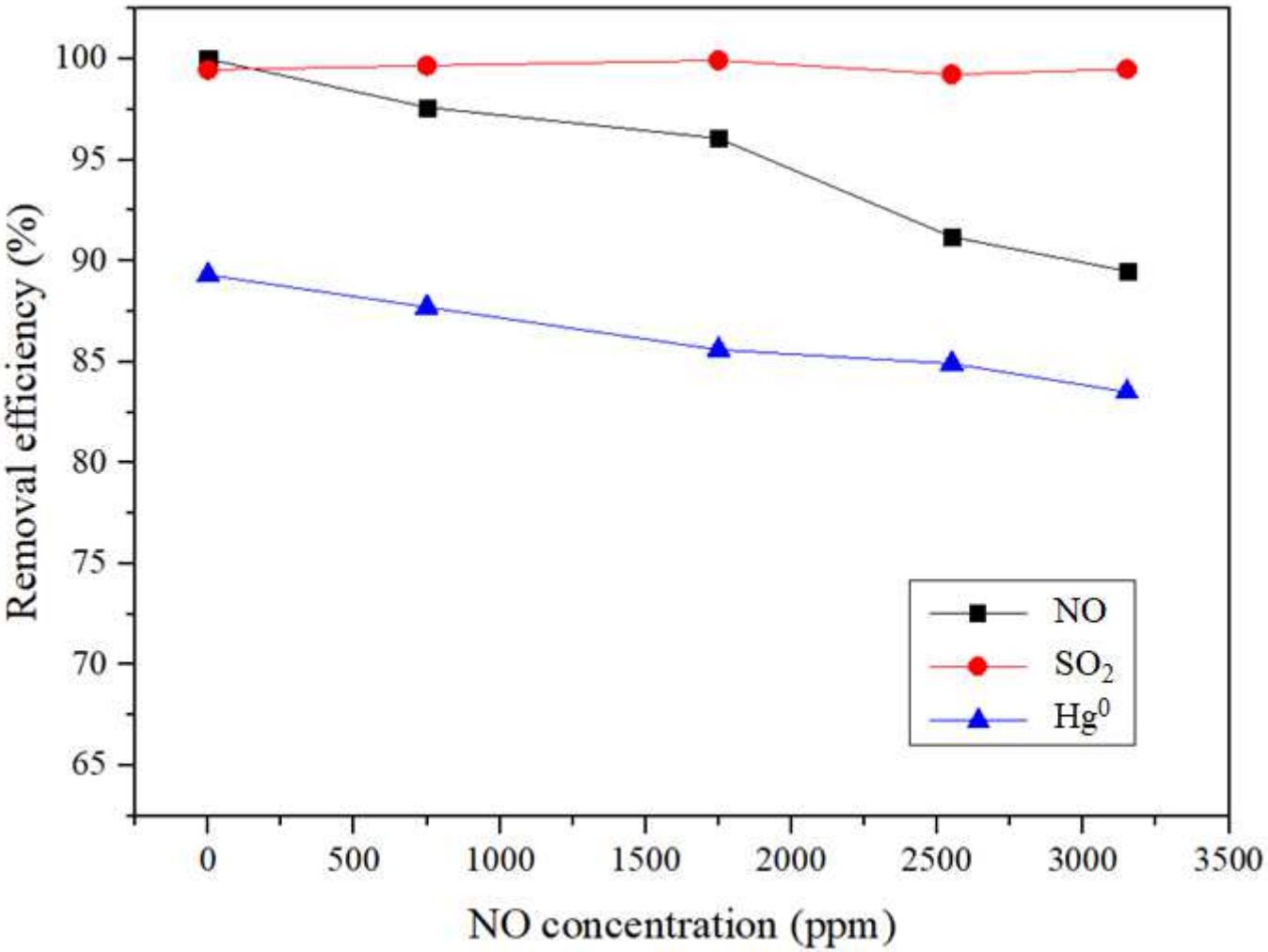

Figure 5

Effects of the NO concentration on the simultaneous removal efficiencies of NO, SO2 and Hg0. Experimental conditions: 3 g/L urea; initial solution pH, 7.46; initial solution temperature, 298 K; 2750 ppm SO2; and Hg0 penetration rate, 150 ng/min.

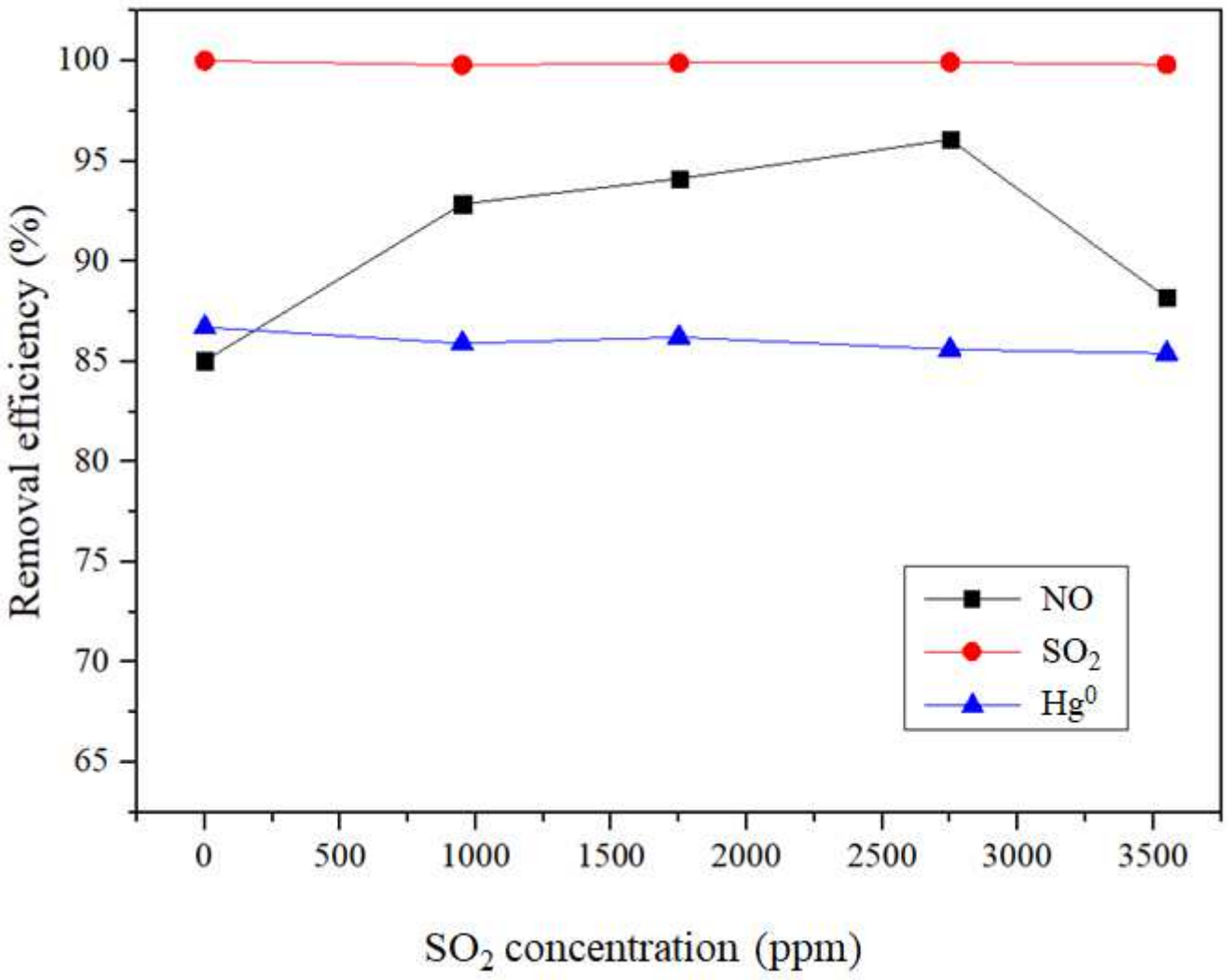

Figure 6

Effects of the SO2 concentration on the simultaneous removal efficiencies of NO, SO2 and Hg0. Experimental conditions: 3 g/L urea; initial solution pH, 7.46; initial solution temperature, 298 K; 1750 ppm NO; and Hg0 penetration rate, 150 ng/min.

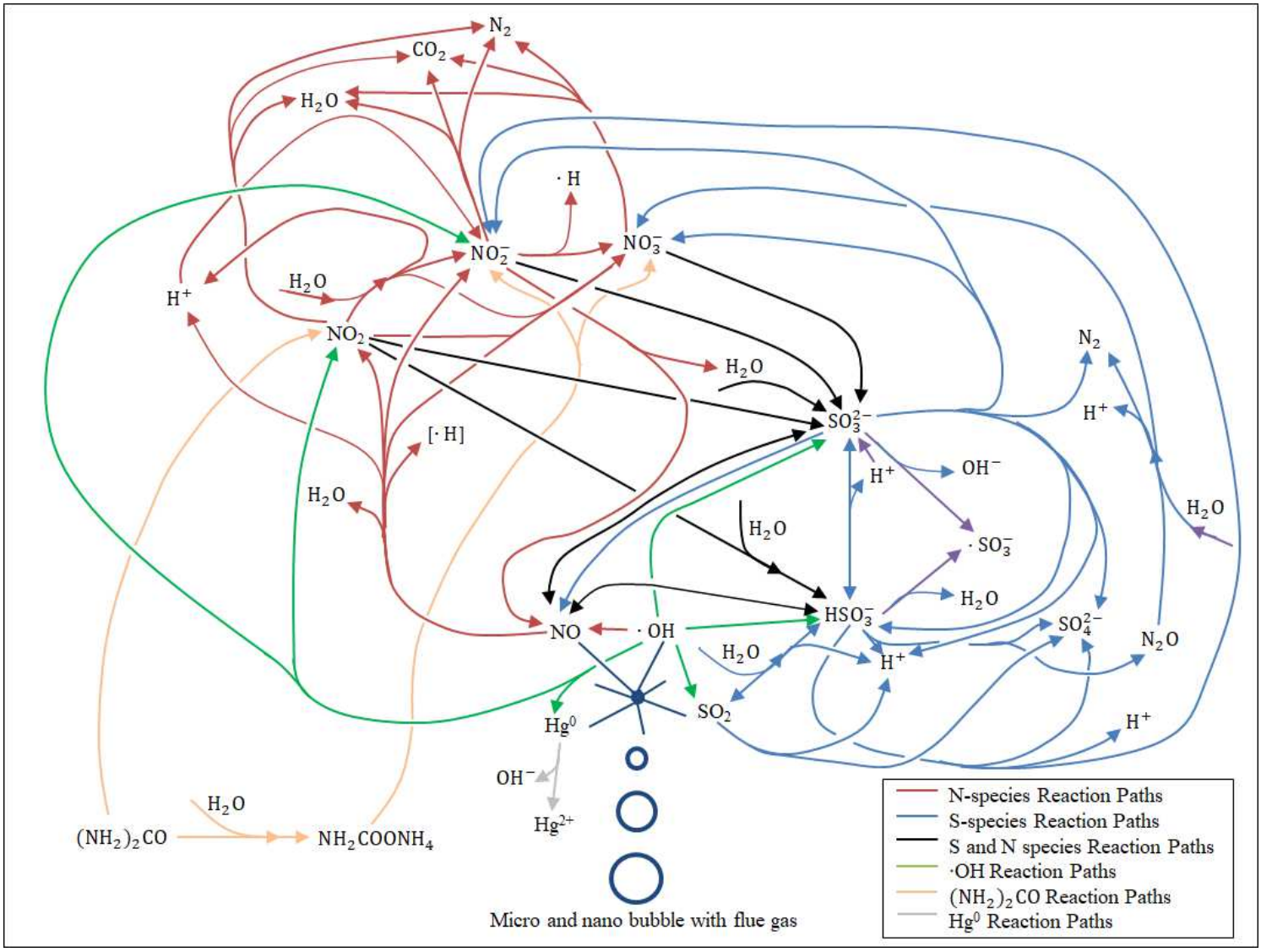

Figure 7

Schematic diagram of the reaction mechanism

Supplementary Files

This is a list of supplementary files associated with this preprint. Click to download.

- Supplementarymaterials.docx